Ab initio evaluation of Coulomb and exchange parameters for DFT+U calculations

Nicholas J. Mosey and Emily A. Carter*

Department of Mechanical and Aerospace Engineering and Program in Applied and Computational Mathematics, Princeton University, Princeton, New Jersey 08544-5263, USA

(Received 15 March 2007; revised manuscript received 18 June 2007; published 25 October 2007)

Conventional density functional theory (DFT) fails for materials with strongly correlated electrons, such as late transition metal oxides. Large errors in the intra-atomic Coulomb and exchange interactions are the source of this failure. The DFT+U method has provided a means, through empirical parameters, to correct these errors. Here, we present a systematic *ab initio* approach in evaluating the intra-atomic Coulomb and exchange terms, U and J, respectively, in order to make the DFT+U method a fully first-principles technique. The method is based on a relationship between these terms and the Coulomb and exchange integrals evaluated in the basis of unrestricted Hartree-Fock molecular orbitals that represent localized states of the extended system. We used this *ab initio* scheme to evaluate U and J for chromia (Cr_2O_3). The resulting values are somewhat higher than those determined earlier either empirically or in constrained DFT calculations but have the advantage of originating from an *ab initio* theory containing exact exchange. Subsequent DFT+U calculations on chromia using the *ab initio* derived U and J yield properties consistent with experiment, unlike conventional DFT. Overall, the technique developed and tested in this work holds promise in enabling accurate and fully predictive DFT+U calculations of strongly correlated electron materials.

DOI: 10.1103/PhysRevB.76.155123 PACS number(s): 71.27.+a, 71.15.Mb

I. INTRODUCTION

The advent of Kohn-Sham density functional theory[1–5] (DFT) in conjunction with rapid advances in computer technology has enabled accurate first-principles simulations of systems containing hundreds of atoms. These calculations have contributed to the development of a better understanding of the fundamental properties of molecules and materials, leading to the emergence of simulation as a powerful tool for obtaining information that is difficult, or even impossible, to acquire experimentally. Despite the success of DFT, there still exist classes of systems and phenomena for which current forms of the theory fail not just quantitatively but even qualitatively (e.g., predicting a known insulator to be metallic). As usual, this is due primarily to the use of approximate exchange-correlation (XC) functionals. Accurate first-principles calculations of such systems must await the development of computationally efficient methods that capture the essential physics missing in approximate XC functionals. The development of such techniques is an active area of research.

An important class of materials poorly described by conventional DFT [i.e., DFT within the local density approximation (LDA) or the generalized gradient approximation (GGA) to electron exchange and correlation] is that of strongly correlated electron materials (SCEMs). SCEMs include actinides and middle-to-late transition metal oxides, which contain many electrons in partially filled d or f shells. The d and f electrons are inherently localized on each metal atom, and the associated intra-atomic exchange and Coulomb energy terms are both numerous and large, due the many electrons and the localized, tight nature of the wave functions involved. Since conventional DFT with approximate exchange and correlation does not properly cancel out the spurious electron self-interaction, the electron-electron repulsion is predicted to be far too large. As a result, the electrons in conventional DFT calculations incorrectly delocalize to reduce the repulsion energy, which converts what should be an insulator (e.g., in the case of transition metal oxides) to a metal.

A suitable theoretical treatment of SCEMs thus rests on the ability to accurately account for self-interaction energies, especially those arising from electrons in localized states. Hartree-Fock (HF) theory provides a natural framework for this because HF calculations contain exact exchange and, hence, are free of self-interaction by design. Unfortunately, the absence of static and dynamic correlation effects in HF calculations renders this method unsuitable for predictive simulations. Well-known extensions of HF theory exist that account for electron correlation; however, these methodologies are very expensive computationally and, for the most part, have not been implemented for extended crystals.[6,7]

Recently, the search for an electronic structure method that is computationally efficient, largely free of self-interaction error, and accounts for a degree of dynamic correlation has focused on combining various methods that meet at least one of these criteria. In these approaches, the electronic structure is divided into localized and delocalized states, and each electronic subsystem is treated with an appropriate electronic structure method. Such hybrid approaches are motivated from model Hamiltonian techniques, such as the Hubbard U[8,9] and Anderson impurity[10] models, which have been used historically to treat SCEMs in an empirical fashion.

Currently, the hybrid technique used most frequently to study SCEMs is known as DFT+U.[11,12] In this theory, the interactions between electrons in states localized on the same atomic center (called on-site interactions) are treated in an HF-like manner, while the remaining interactions are treated with DFT. This makes great physical sense because the errors incurred by DFT are largely due to the intra-atomic self-interaction error, which should be well corrected by an HF description. In practice, the on-site interaction energy is evaluated with a parametrized Hamiltonian instead of an ex-

plicit HF calculation. The parameters that enter into this Hamiltonian correspond to the average Coulomb and exchange interactions between electrons of the same angular momentum that are localized on the same atom. These parameters are designated as $U_{I\ell}$ and $J_{I\ell}$, respectively, where I designates the atomic center on which the electrons are localized and ℓ denotes their angular momentum. The key to performing an accurate DFT+U calculation lies in selecting suitable values for these parameters. Two methods are commonly used in this respect. In one case, these values are treated as tunable parameters, which are chosen to reproduce known properties of the system of interest.[13,14] This empirical approach often may be reasonable but lacks a theoretical basis, is subject to bias from using a limited amount of data to select the parameters, and is not applicable in cases where experimental data are limited or nonexistent. In the other case, constrained DFT calculations[15,16] are performed in which the number of electrons in states localized on a particular atomic site is fixed while the remainder of the electronic structure is relaxed. By monitoring the change in the total energy as a function of the number of localized electrons, it is possible to extract values for $U_{I\ell}$ and $J_{I\ell}$ from these calculations while accounting for screening effects from the remainder of the system. Although this approach is motivated from first principles, the calculated values are of questionable accuracy due to the artificial nature of the constrained systems, the inherent inaccuracy of the DFT exchange-correlation functionals for localized, open-shell electronic states (as discussed above), and the observed significant dependence of the calculated values of $U_{I\ell}$ and $J_{I\ell}$ on the basis set used in such calculations.

In the present work, a means of evaluating $U_{I\ell}$ and $J_{I\ell}$ from unrestricted HF (UHF) calculations is developed and assessed. This *ab initio* approach is not subject to the difficulties and potential bias associated with using limited amounts of experimental data, as in empirical parameter fitting, and although UHF calculations do not capture static and dynamic correlation effects, they do not suffer from the self-interaction errors that are present in constrained DFT calculations. As such, this approach may prove to be an effective means of unambiguously determining these parameters from first principles for use in subsequent DFT+U calculations, offering a fully predictive DFT+U theory. The method developed in this work is based on an approximate relationship between the parameters $U_{I\ell}$ and $J_{I\ell}$ and the Coulomb and exchange integrals evaluated in the basis of the UHF molecular orbitals corresponding to the localized states of the system. These integrals are evaluated by performing UHF calculations on embedded cluster models that represent the bulk material of interest and yield approximate values for the true interactions between the localized electrons in the real material. The values of $U_{I\ell}$ and $J_{I\ell}$ obtained in this approach are treated as constants for the material and do not depend on the exchange-correlation functional to be used in the DFT+U calculation. Due to the lack of static and dynamic correlation effects in UHF calculations, the values of $U_{I\ell}$ and $J_{I\ell}$ derived from this method are upper bounds on the true strengths of these interactions. The results of test calculations on chromia (Cr_2O_3) demonstrate that converged *ab initio* values of $U_{I\ell}$ and $J_{I\ell}$ can be obtained with clusters and basis sets that are modest in size, with the primary requisite for convergence being a model that provides an adequate description of the slight delocalization of the "localized" states over neighboring atoms. The converged values of $U_{I\ell}$ and $J_{I\ell}$ evaluated in these cluster calculations are similar to those determined previously with empirical and constrained DFT techniques, but we believe that the *ab initio* values rest on a firmer theoretical footing. Subsequent DFT+U calculations of bulk chromia performed with the *ab initio* values of $U_{I\ell}$ and $J_{I\ell}$ yield results in very good agreement with experiments. This indicates that the developed methodology may be a powerful means of obtaining reliable estimates of $U_{I\ell}$ and $J_{I\ell}$ for use in DFT+U calculations of other SCEMs.

The remainder of this paper is as follows. A brief overview of the DFT+U method is provided in Sec. II. The *ab initio* evaluation of $U_{I\ell}$ and $J_{I\ell}$ is described in Sec. III and applied in Sec. IV to determine parameters for chromia. DFT+U calculations of bulk chromia are presented in Sec. V to assess the quality of the *ab initio* parameters, and the conclusions are given in Sec. VI.

II. DFT+U METHODOLOGY

The DFT+U method has been described in detail elsewhere,[11,12] and only a brief introduction will be provided here. The technique is based on the use of HF theory to evaluate the on-site interactions between localized electrons and the use of DFT to calculate all other electronic terms. This is achieved through the following total energy functional:

$$E^{DFT+U}[\rho,\{n_{I\ell m\sigma}\}] = E^{DFT}[\rho] + E^{on\text{-}site}[\{n_{I\ell m\sigma}\}] - E^{dc}[\{n_{I\ell\sigma}\}], \tag{1}$$

where E^{DFT+U} is the total energy of the system, E^{DFT} is the DFT energy of the system based on the total electron density ρ, $E^{on\text{-}site}$ is the HF energy arising from on-site interactions between localized electrons, and E^{dc} is a double-counting term which corrects for contributions to the total energy that are included in both E^{DFT} and $E^{on\text{-}site}$. The on-site interaction energy $E^{on\text{-}site}$ is dependent on the number of electrons that occupy localized orbitals $\varphi_{I\ell m\sigma}$, which are centered on atom I and characterized by angular momentum ℓ, magnetic quantum number m, and spin σ. These atom-centered, localized orbitals consist of spherical harmonics multiplied by a radial function selected to accurately represent the electronic states of the spheridized non-spin-polarized atom. The occupation numbers $n_{I\ell m\sigma}$ are obtained by projecting the Kohn-Sham DFT orbitals for the total system onto a set of these localized orbitals. The value $N_{I\ell\sigma}$ that enters into E^{dc} corresponds to the total number of electrons of a given spin and angular momentum that are localized on I, i.e., $N_{I\ell\sigma}=\Sigma_m n_{I\ell m\sigma}$.

Evaluating the energy with Eq. (1) requires expressions for $E^{on\text{-}site}$ and E^{dc}. Many different forms of these expressions have been proposed in the literature. Here, we will focus on the rotationally invariant approach proposed by Dudarev *et al.*,[17] which was employed in the DFT+U calculations discussed below. In this approach, these quantities are expressed as

$$E^{on\text{-}site}[\{n_{I\ell m\sigma}\}] = \sum_{I,\ell}\left[\left(\sum_{m,m'} n_{I\ell m\alpha}n_{I\ell m'\beta} + \sum_{m,m'>m} n_{I\ell m\alpha}n_{I\ell m'\alpha} + \sum_{m,m'>m} n_{I\ell m\beta}n_{I\ell m'\beta}\right)U_{I\ell}\right] - \sum_{I,\ell}\left[\left(\sum_{m,m'>m} n_{I\ell m\alpha}n_{I\ell m'\alpha} + \sum_{m,m'>m} n_{I\ell m\beta}n_{I\ell m'\beta}\right)J_{I\ell}\right] \quad (2)$$

and

$$E^{dc}[\{N_{I\ell\sigma}\}] = \sum_{I,\ell}\left[\left(N_{I\ell\alpha}N_{I\ell\beta} + \frac{N_{I\ell\alpha}(N_{I\ell\alpha}-1)}{2} + \frac{N_{I\ell\beta}(N_{I\ell\beta}-1)}{2}\right)U_{I\ell}\right] - \sum_{I,\ell}\left[\left(\frac{N_{I\ell\alpha}(N_{I\ell\alpha}-1)}{2} + \frac{N_{I\ell\beta}(N_{I\ell\beta}-1)}{2}\right)J_{I\ell}\right], \quad (3)$$

where the limits on the summations are such that each on-site interaction is counted only once. It is important to note that these expressions only account for interactions between electrons that are localized on the same atomic site and have the same angular momentum. Justifications for these expressions of $E^{on\text{-}site}$ and E^{dc} have been provided elsewhere,[17–20] but essentially, they enumerate the allowed pairwise interactions. For Coulomb terms $U_{I\ell}$, this corresponds to all pairwise interactions between all electrons of the same angular momentum on each site, while for exchange terms $J_{I\ell}$, only pairwise interactions between electrons of the same spin on each site are nonzero.

Inserting Eqs. (2) and (3) into Eq. (1) yields the following total energy functional[17]

$$E^{DFT+U}[\rho,\{n_{I\ell m\sigma}\}] = E^{DFT}[\rho] + \sum_{I,\ell,m,\sigma}\frac{(U_{I\ell}-J_{I\ell})}{2}(n_{I\ell m\sigma}-n_{I\ell m\sigma}^2). \quad (4)$$

The first term on the right hand side of this equation corresponds to the DFT energy obtained using the total electron density ρ and includes the on-site interactions, albeit calculated with conventional DFT, which is known to be inaccurate in this respect. The second term on the right hand side of Eq. (4) corrects for this behavior in the following sense. Note that $U_{I\ell}$ and $J_{I\ell}$ are positive and $n_{I\ell m\sigma}$ lies between 0 and 1. Effectively, the second term then serves as a penalty function that drives the system toward electron densities in which the localized states $\varphi_{I\ell m\sigma}$ have occupation numbers of either 0 or 1. This counters the tendency of DFT calculations to overdelocalize these electronic states and leads to an improved description of the electronic structure. In particular, the energies of the localized states will be shifted from their DFT values such that the band gap is increased, which increases the insulating character of the system. This can be seen if one evaluates the orbital energies by differentiating Eq. (4) with respect to the orbital occupation numbers, which demonstrates that the occupied states are shifted to lower energies while the unoccupied states are shifted to higher energies.

In order to employ Eq. (4), one must provide values for $U_{I\ell}$ and $J_{I\ell}$. These values are not known *a priori* and are system dependent. Thus, the challenge in performing meaningful DFT+U calculations lies in selecting appropriate values for these parameters. As noted above, this is typically achieved through either empirical fitting or constrained DFT calculations, both of which suffer from significant shortcomings. In the next section, an approach will be outlined for evaluating these parameters through *ab initio* UHF calculations.

III. *AB INITIO* EVALUATION OF *U* AND *J*

As discussed in the preceding section, DFT+U calculations employ a parametrized Hamiltonian to evaluate the on-site interaction energy $E^{on\text{-}site}$ between electrons in localized states. In what follows, a means of systematically calculating the parameters used to evaluate $E^{on\text{-}site}$ is developed. This approach involves performing a UHF calculation on the material and calculating the two-electron energy arising from interactions between electrons occupying molecular orbitals (MOs) localized on the same atom. The starting point for this approach is to write the two-electron UHF energy E^{UHF} for a set of MOs $\{\phi_i^{\sigma_i}\}$:

$$E^{UHF}[\{\phi_i^{\sigma_i}\}] = \sum_{i,j} C_{ij}^{\alpha\beta} + \sum_{i,j>i} C_{ij}^{\alpha\alpha} + \sum_{i,j>i} C_{ij}^{\beta\beta} - \sum_{i,j>i} X_{ij}^{\alpha\alpha} - \sum_{i,j>i} X_{ij}^{\beta\beta},$$

$$C_{ij}^{\sigma_i\sigma_j} = \int\int \frac{\phi_i^{\sigma_i}(\mathbf{r}_1)\phi_i^{\sigma_i}(\mathbf{r}_1)\phi_j^{\sigma_j}(\mathbf{r}_2)\phi_j^{\sigma_j}(\mathbf{r}_2)}{|\mathbf{r}_1-\mathbf{r}_2|}d\mathbf{r}_1 d\mathbf{r}_2,$$

$$X_{ij}^{\sigma_i\sigma_j} = \int\int \frac{\phi_i^{\sigma_i}(\mathbf{r}_1)\phi_j^{\sigma_j}(\mathbf{r}_1)\phi_j^{\sigma_j}(\mathbf{r}_2)\phi_i^{\sigma_i}(\mathbf{r}_2)}{|\mathbf{r}_1-\mathbf{r}_2|}d\mathbf{r}_1 d\mathbf{r}_2, \quad (5)$$

where $C_{ij}^{\sigma_i\sigma_j}$ and $X_{ij}^{\sigma_i\sigma_j}$ represent Coulomb and exchange integrals involving UHF canonical MOs i and j, which are occupied by electrons with spins σ_i and σ_j, respectively. An unconventional notation has been employed in Eq. (5) to avoid confusion with terms used earlier (conventionally, Coulomb integrals would be designated with U or J and exchange integrals would be labeled as J or K).

E^{UHF} is the HF energy arising from all two-electron interactions in the system. Meanwhile, $E^{on\text{-}site}$ only includes interactions between electrons of the same angular momentum that are localized on the same atom. In order to extract the on-site energy from Eq. (5), it will prove useful to recognize that, in principle, it is possible to decompose the occupation numbers of the UHF MOs into contributions from atomic orbitals of well-defined angular momentum that are centered

on specific atoms. That is, the occupation number of orbital $\phi_i^{\sigma_i}$ can be expressed as $N_{i\sigma}=\Sigma_{I,\ell}n_{I\ell i\sigma}$, where $n_{I\ell i\sigma}$ designates the contribution to the MO of electrons with spin σ residing in atomic orbitals of angular momentum ℓ centered on atom I. The values of $n_{I\ell i\sigma}$ can be obtained by projecting the UHF canonical MOs onto a set of atom-centered basis functions that have well-defined values of I and ℓ.

Since $N_{i\sigma}=1$ for occupied states, it is valid to rewrite Eq. (5) as

$$\begin{aligned}E^{UHF}=&\sum_{i,j}\left(\sum_{I,\ell}n_{I\ell i\alpha}\sum_{I',\ell'}n_{I'\ell'j\beta}C_{ij}^{\alpha\beta}\right)\\&+\sum_{i,j>i}\left(\sum_{I,\ell}n_{I\ell i\alpha}\sum_{I',\ell'}n_{I'\ell'j\alpha}C_{ij}^{\alpha\alpha}\right)\\&+\sum_{i,j>i}\left(\sum_{I,\ell}n_{I\ell i\beta}\sum_{I',\ell'}n_{I'\ell'j\beta}C_{ij}^{\beta\beta}\right)\\&-\sum_{i,j>i}\left(\sum_{I,\ell}n_{I\ell i\alpha}\sum_{I',\ell'}n_{I'\ell'j\alpha}X_{ij}^{\alpha\alpha}\right)\\&-\sum_{i,j>i}\left(\sum_{I,\ell}n_{I\ell i\beta}\sum_{I',\ell'}n_{I'\ell'j\beta}X_{ij}^{\beta\beta}\right).\end{aligned}\tag{6}$$

If we retain in Eq. (6) only the terms corresponding to the on-site interactions between electrons with the same angular momentum, i.e., those where $I=I'$ and $\ell=\ell'$, we obtain

$$\begin{aligned}E_{on\text{-}site}^{UHF}=&\sum_{I,\ell}\left(\sum_{i,j}n_{I\ell i\alpha}n_{I\ell j\beta}C_{ij}^{\alpha\beta}+\sum_{i,j>i}n_{I\ell i\alpha}n_{I\ell j\alpha}C_{ij}^{\alpha\alpha}\right.\\&\left.+\sum_{i,j>i}n_{I\ell i\beta}n_{I\ell j\beta}C_{ij}^{\beta\beta}\right)-\sum_{I,\ell}\left(\sum_{i,j>i}n_{I\ell i\alpha}n_{I\ell j\alpha}X_{ij}^{\alpha\alpha}\right.\\&\left.+\sum_{i,j>i}n_{I\ell i\beta}n_{I\ell j\beta}X_{ij}^{\beta\beta}\right),\end{aligned}\tag{7}$$

which corresponds to the two-electron energy arising from on-site interactions between electrons in atomic orbitals of the same angular momentum ℓ that are centered on the same atom I. If one restricts I and ℓ to values consistent with the localized electrons in the system and restricts i and j to UHF MOs that are composed primarily of atomic basis functions of angular momentum ℓ that are centered on I, i.e., the UHF MOs that correspond to the localized states, it is possible to define $E_{on\text{-}site}^{UHF}$ as the on-site energy of interest in DFT+U calculations. Setting $E^{on\text{-}site}=E_{on\text{-}site}^{UHF}$, with the appropriate restrictions on I, ℓ, i, and j, forms the basis for evaluating $U_{I\ell}$ and $J_{I\ell}$ from the Coulomb and exchange integrals evaluated in the basis of localized canonical UHF MOs.[21]

In order to obtain expressions for $U_{I\ell}$ and $J_{I\ell}$ from Eq. (7), a weighting factor, $n_{I\ell i\sigma_i}n_{I\ell j\sigma_j}$, is assigned to each Coulomb and exchange integral. The Coulomb and exchange terms in Eq. (7) are then multiplied and divided by the sum of these factors to yield

$$\begin{aligned}E_{on\text{-}site}^{UHF}[\{\phi_{i\sigma}\},\{n_{I\ell i\sigma}\}]=&\sum_{I,\ell}\left[\left(\sum_{i,j}n_{I\ell i\alpha}n_{I\ell j\beta}+\sum_{i,j>i}n_{I\ell i\alpha}n_{I\ell j\alpha}+\sum_{i,j>i}n_{I\ell i\beta}n_{I\ell j\beta}\right)\right.\\&\left.\times\left(\frac{\sum_{i,j}n_{I\ell i\alpha}n_{I\ell j\beta}C_{ij}^{\alpha\beta}+\sum_{i,j>i}n_{I\ell i\alpha}n_{I\ell j\alpha}C_{ij}^{\alpha\alpha}+\sum_{i,j>i}n_{I\ell i\beta}n_{I\ell j\beta}C_{ij}^{\beta\beta}}{\sum_{i,j}n_{I\ell i\alpha}n_{I\ell j\beta}+\sum_{i,j>i}n_{I\ell i\alpha}n_{I\ell j\alpha}+\sum_{i,j>i}n_{I\ell i\beta}n_{I\ell j\beta}}\right)\right]\\&-\sum_{I,\ell}\left[\left(\sum_{i,j>i}n_{I\ell i\alpha}n_{I\ell j\alpha}+\sum_{i,j>i}n_{I\ell i\beta}n_{I\ell j\beta}\right)\left(\frac{\sum_{i,j>i}n_{I\ell i\alpha}n_{I\ell j\alpha}X_{ij}^{\alpha\alpha}+\sum_{i,j>i}n_{I\ell i\beta}n_{I\ell j\beta}X_{ij}^{\beta\beta}}{\sum_{i,j>i}n_{I\ell i\alpha}n_{I\ell j\alpha}+\sum_{i,j>i}n_{I\ell i\beta}n_{I\ell j\beta}}\right)\right].\end{aligned}\tag{8}$$

This expression is similar to that in Eq. (2). Specifically, within each of the brackets, there exists a summation over products of occupation numbers multiplied by an expression representing the average on-site Coulomb or exchange energies. Equating Eq. (2) with Eq. (8) and setting $n_{I\ell i\sigma}=n_{I\ell m\sigma}$ lead to the following expressions for $U_{I\ell}$ and $J_{I\ell}$:

$$U_{I\ell}=\frac{\sum_{i,j}n_{I\ell i\alpha}n_{I\ell j\beta}C_{ij}^{\alpha\beta}+\sum_{i,j>i}n_{I\ell i\alpha}n_{I\ell j\alpha}C_{ij}^{\alpha\alpha}+\sum_{i,j>i}n_{I\ell i\beta}n_{I\ell j\beta}C_{ij}^{\beta\beta}}{\sum_{i,j}n_{I\ell i\alpha}n_{I\ell j\beta}+\sum_{i,j>i}n_{I\ell i\alpha}n_{I\ell j\alpha}+\sum_{i,j>i}n_{I\ell i\beta}n_{I\ell j\beta}},$$

$$J_{I\ell}=\frac{\sum_{i,j>i}n_{I\ell i\alpha}n_{I\ell j\alpha}X_{ij}^{\alpha\alpha}+\sum_{i,j>i}n_{I\ell i\beta}n_{I\ell j\beta}X_{ij}^{\beta\beta}}{\sum_{i,j>i}n_{I\ell i\alpha}n_{I\ell j\alpha}+\sum_{i,j>i}n_{I\ell i\beta}n_{I\ell j\beta}}.\tag{9}$$

These expressions relate $U_{I\ell}$ and $J_{I\ell}$ to the localized canonical MOs obtained in a UHF calculation, thereby providing an *ab initio* means of evaluating the parameters required for DFT+U calculations.

It can be shown that Eq. (2) is equal to Eq. (8) only if it is possible to transform the subset of canonical UHF MOs used to evaluate the Coulomb and exchange integrals into a form where each orbital can be mapped onto an atomiclike orbital with distinct values of I, ℓ, m, and σ. Values of $U_{I\ell}$ and $J_{I\ell}$ are invariant to such rotations provided that the transformation is applied to orbitals of the same symmetry. If, for some reason, the UHF orbitals used to calculate $U_{I\ell}$ and $J_{I\ell}$ could not be represented in a form where only one MO corresponds to a given value of m, the calculated values of $U_{I\ell}$ and $J_{I\ell}$ would contain contributions from electrons defined by the same values of I, ℓ, m, and σ, which are not included in the definition of $E^{on\text{-}site}$ in Eq. (2). This requirement cannot be strictly met—even for localized states of interest in DFT+U calculations—due to the delocalized nature of UHF MOs. However, in practice, the fact that the canonical UHF MOs of interest are highly concentrated on specific atoms and the requirement that the MOs remain orthogonal is sufficient to ensure that MOs of the same spin that are characteristic of the same angular momentum and concentrated on the same atom will be projected primarily onto spherical harmonic basis functions with different values of m. Thus, while this is an approximation that is inherent to the method outlined above, it is relatively minor for systems with localized states appropriate for studying with DFT+U methods.

Another approximation inherent to the method involves the evaluation of the occupation numbers $n_{I\ell i\sigma}$, as there does not exist an exact means of dividing the occupation number of an MO into contributions from orbitals of a specific angular momentum located on a specific atomic center. In practice, this decomposition is achieved by projecting each MO onto a set of atom-centered basis functions, which are composed of a set of spherical harmonics multiplied by appropriate radial functions. Thus, the occupation numbers will ultimately be dependent on the nature of these radial functions. Fortunately, the localized UHF MOs used to evaluate any particular values of $U_{I\ell}$ and $J_{I\ell}$ will be projected onto basis functions with the same value of I and ℓ and, hence, will be subjected consistently to any variations in the radial components. That is, if the radial function used in conjunction with spherical harmonics of angular momentum ℓ localized on atom I is changed such that the occupation number $n_{I\ell i\sigma}$ associated with one of the localized UHF MOs is decreased by one-half, the occupation numbers of the other localized MOs associated with the same angular momentum and atomic center will also be reduced by approximately one-half. Furthermore, the similarities between the localized UHF MOs associated with specific values of I and ℓ ensure that the occupation numbers associated with these MOs will also be similar to one another. Thus, the occupation numbers associated with the MOs will be similar to one another and will scale uniformly with the basis functions onto which they are projected. It can be demonstrated that if these conditions are met, the variations in the occupations numbers with the basis set will cancel when $U_{I\ell}$ and $J_{I\ell}$ are calculated with the expressions in Eq. (9), and, hence, the calculated values of $U_{I\ell}$ and $J_{I\ell}$ will be relatively insensitive to changes in the basis set used to evaluate the occupation numbers. Numerical tests given below will demonstrate this assertion.

IV. COULOMB AND EXCHANGE PARAMETERS FOR CHROMIA

In the preceding section, an approach was developed for evaluating $U_{I\ell}$ and $J_{I\ell}$ from the set of canonical UHF MOs representing the localized states in a strongly correlated system. In this section, this scheme will be used to determine values of $U_{I\ell}$ and $J_{I\ell}$ for chromia. Since the only localized electrons in chromia reside in the d states of the chromium atoms ($\ell=2$ and $I=$Cr), the subscripts on $U_{I\ell}$ and $J_{I\ell}$ will be dropped in what follows. Furthermore, efforts will focus on determining $(U-J)$, which is the relevant quantity in the DFT+U energy functional in Eq. (4). The details of the UHF calculations are given in Sec. IV A, and the results are discussed in Sec. IV B.

A. Details of the unrestricted Hartree-Fock calculations

1. Model systems

The repulsion between electrons in orbitals localized on a specific atomic center is highly influenced by the environment around that atom. This is primarily due to screening effects which reduce the repulsive interactions between these electrons. Indeed, preliminary UHF calculations on individual Cr ions, i.e., neglecting all screening from the environment, yielded values of $(U-J)$ that were between 17 and 23 eV, depending on the ionic charge. Meanwhile, typical values of $(U-J)$ used in calculations of transition metal oxides are in the range of 2–10 eV,[22] with a value of 4 eV for chromia being determined empirically in a previous study.[14] The large differences between the values obtained in the isolated ion calculations and those determined (either empirically or with constrained DFT calculations) for extended systems highlight the need to incorporate environmental aspects into the calculation of $(U-J)$.

In order to include screening effects, calculations were performed on finite-sized Cr_xO_y clusters embedded in a field of point charges representing bulk chromia. The clusters were constructed by starting with a single CrO_6^{9-} unit (consistent with the formal oxidation states of Cr and O in chromia of Cr^{3+} and O^{2-}) and adding successive shells of Cr^{3+} ions along with enough O^{2-} ions to ensure that each chromium was surrounded by a total of six oxygens. Altogether, clusters containing between seven atoms (CrO_6^{9-}) and 63 atoms ($Cr_{15}O_{48}^{51-}$) were considered. The positions of the atoms in these clusters corresponded to those in the experimental geometry of bulk chromia. The influence of the size of the embedded cluster on the calculated values of $(U-J)$ is discussed below.

The clusters were embedded in a set of point charges with positions corresponding to the locations of Cr and O atoms in an $8\times8\times2$ representation of the experimental hexagonal unit cell of Cr_2O_3, where $8\times8\times2$ refers to the number of repeated hexagonal unit cells along each lattice vector. The system was only repeated twice along the last direction due

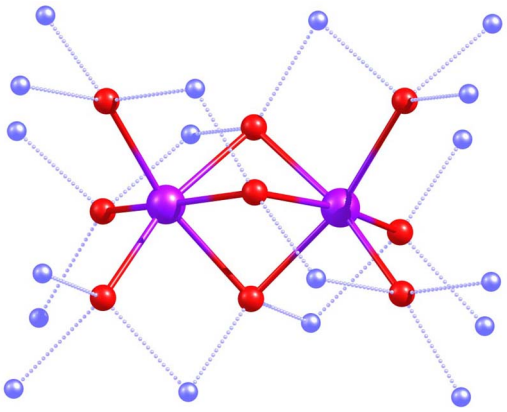

FIG. 1. (Color online) One of the clusters considered in this study. The $Cr_2O_9^{12-}$ cluster is surrounded by a set of Al PP cores, and the whole cluster is embedded in a series of point charges corresponding to an $8\times8\times2$ representation of the experimental hexagonal unit cell of chromia. This set of point charges is not shown. Chromium atoms are purple, oxygen atoms are red, and point charges represented by Al PPs are pale blue. Solid lines indicate bonds within the cluster, and dotted lines designate interactions between the Al PPs and the outer oxygen atoms of the cluster.

to the increased length of the associated lattice vector. Altogether, this model contains a total of approximately 4000 point charges, depending on the specific cluster under consideration, and provides an approximately isotropic representation of the point charges about the central position of the point charge field where the embedded cluster was placed. Test calculations demonstrated that the distance between the outermost atoms of the embedded cluster and the outer edge of the point charge field (at least 8 Å) was sufficient to yield converged values of $(U-J)$. The points at the locations of Cr atoms were assigned charges of $+3e$, while those at the positions of O atoms were assigned charges of $-2e$. The point charges at the locations of Cr ions nearest to the embedded cluster were represented by Al pseudopotentials (PPs),[23] which have a net charge of $+3e$. The purpose of the PPs is to act as a barrier between the cluster and the set of point charges, which prevents the unphysical drift of electron density from the outer oxygen atoms of the cluster into the point charge field. This is achieved with PPs because they provide a degree of exchange repulsion which effectively contains the electron density within the region associated with the embedded cluster. This approach has been used extensively in embedded cluster calculations.[24–27] An example of one of the clusters considered in these calculations surrounded by the set of PPs is shown in Fig. 1.

2. Electronic structure calculations

Chromia is an antiferromagnetic material in which the net spin on a given chromium atom is the opposite of that on its neighboring four Cr atoms.[28–30] Obtaining an antiferromagnetic electronic structure is a challenging task in quantum chemical calculations, particularly for large systems in which one must control the net spin at many atomic sites. However, an accurate representation of the electronic structure is critical for evaluating reliable values of $(U-J)$. In this work, the following approach was employed to generate electronic structures consistent with the experimental antiferromagnetic spin ordering of chromia. First, a UHF calculation was performed with the system in a ferromagnetic state, and the resulting canonical UHF MOs were localized according to the procedure of Pipek and Mezey.[31] Analysis of the localized MOs permitted the identification of orbitals that were composed primarily of d-type atomic basis functions centered on an individual Cr atom. The localized MOs were then used to construct the initial guess wave function for a subsequent UHF calculation, with the localized MOs characterized as d states associated with specific Cr atoms being assigned either α or β spin as required to achieve an antiferromagnetic electronic structure. The electronic structure obtained through this second UHF calculation exhibited the correct antiferromagnetic spin ordering. Moreover, a subset of the canonical UHF MOs obtained in this calculation was composed of orbitals that were highly concentrated on specific Cr atoms and exhibited a high degree of d character. An example of a set of these orbitals is shown in Fig. 2.

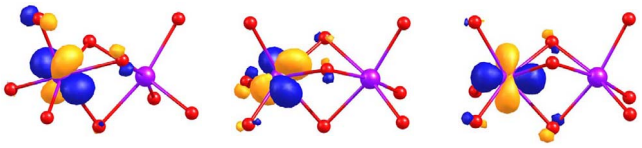

FIG. 2. (Color online) Canonical UHF MOs that are highly localized on one of the Cr atoms of the $Cr_2O_9^{12-}$ cluster. The orbitals are plotted at a contour value of 0.075 a.u. The different colors of the orbitals indicate opposite signs of the wave function. The chromium atoms are colored purple and the oxygens are red. Note that the structures were rotated to clearly illustrate each orbital.

The values of U and J were calculated with the expressions in Eq. (9) using the canonical UHF MOs corresponding to the d states that were localized on the central Cr atom of each Cr_xO_y cluster. In general, there were three of these orbitals, which corresponded to the t_{2g} states of this atom. The orbitals used in the calculations of U and J were restricted to those localized on the central Cr atoms because the environment around this atom will become increasingly bulklike as the cluster size is increased, while the orbitals on the outer Cr atoms experience edge effects and may not be screened properly. The number of d electrons associated with each of the MOs used to evaluate U and J, i.e., the values of $n_{l\ell i\sigma}$ that enter into Eq. (9), were calculated by using the MO coefficients to construct Mulliken populations of the spherical harmonic Gaussian basis functions used in the UHF calculations and summing over populations of all basis functions with the correct values of l and ℓ. This was repeated for each of the three MOs used to evaluate U and J.

The UHF calculations were performed using a version of the GAMESS-US code,[32,33] which we modified to calculate and print out the Coulomb and exchange integrals involving any specific pair of MOs. These individual integrals, evaluated in the MO basis, must be known to calculate U and J with Eq. (9). A series of atom-centered Gaussian basis sets was considered in these calculations to explore the dependence of $(U-J)$ on the basis set size and ensure that a converged value of this quantity was obtained. Three different basis sets

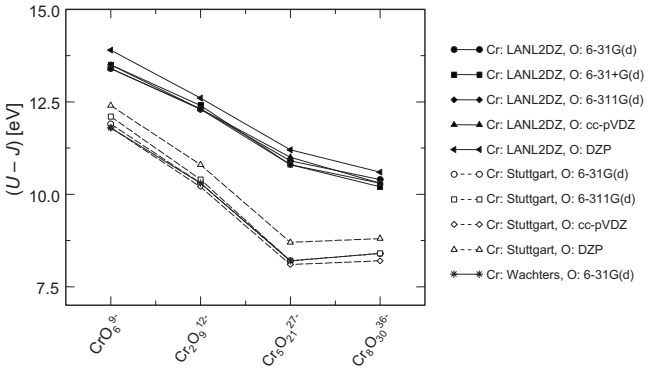

FIG. 3. Dependence of $(U-J)$ on the basis set for a series of Cr_xO_y clusters. The results demonstrate that the calculated value of $(U-J)$ is relatively insensitive to the basis set used on the oxygen atoms yet can be altered significantly by changing the basis set used on chromium.

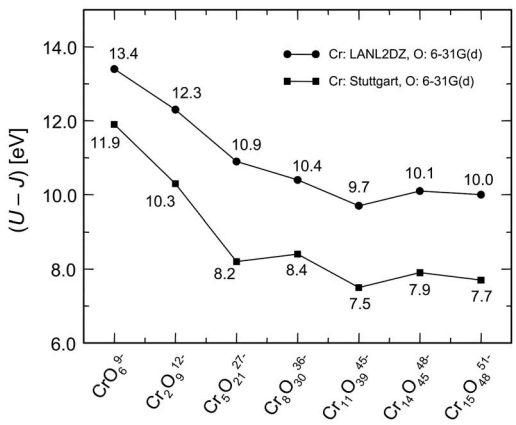

FIG. 4. Dependence of $(U-J)$ on the size of the Cr_xO_y clusters for two different basis sets on Cr and a 6-31G(d) basis set on oxygen. The results demonstrate that converged values of $(U-J)$ are obtained for clusters larger than $Cr_{11}O_{39}^{45-}$. The results obtained with the Stuttgart basis set on Cr demonstrate that a converged value of $(U-J)$ is 7.7 eV.

were used to treat the electrons on the Cr atoms in the embedded cluster. Two of these, the LANL2DZ basis set of Hay and Wadt[23] and the Stuttgart basis set developed by Dolg *et al.*,[34] treated the 3*s*, 3*p*, 3*d*, and 4*s* valence electrons explicitly and represented the remaining ten electrons with a PP. The third was the all-electron basis set of Wachters.[35,36] Five different basis sets were considered for oxygen. These were the well-known 6-31G(d), 6-311G(d), 6-31+G(d), cc-pVDZ, and DZP basis sets.[37–39] The first three basis sets in this series permit an investigation of the effect of systematically altering the basis set on O by increasing the number of valence basis functions or adding diffuse functions, while the latter two allow for a consideration of the effect of employing non-Pople basis sets in the calculations. In all cases, the angular dependence of the basis functions was represented with spherical harmonics, which facilitated the evaluation of the occupation numbers $n_{l\ell i\sigma}$ that enter into Eq. (9) through Mulliken population analysis as described above.

B. Results

The procedure and models described above were used to evaluate $(U-J)$ for chromia. As noted above, the values of U and J were calculated with the expressions in Eq. (9) using canonical UHF MOs that were of high d character and localized on the central Cr atom of the cluster. The dependence of $(U-J)$ on the basis set and cluster size is explored in what follows, along with the requisites for obtaining converged values of this quantity.

Values of $(U-J)$ were calculated using the series of basis sets described above for a small range of cluster sizes. The results of these calculations are summarized in Fig. 3 and show that the data form two groups, which are distinguished by the basis set used on Cr. Specifically, changing the basis set on Cr from LANL2DZ to either of the Stuttgart or Wachters basis sets can alter the calculated value of $(U-J)$ by as much as ~2.5 eV, which is sufficiently large to have a significant effect on the results of a DFT+U calculation. Meanwhile, changing the basis set on O alters the results by 0.5 eV at most, which is sufficiently converged for DFT +U calculations. These observations are true across the range of clusters considered in the calculations.

The results thus indicate that the calculated value of $(U-J)$ is relatively insensitive to the basis set used on O yet is highly dependent on that applied to Cr, which is not particularly surprising, since $(U-J)$ is intrinsically a Cr-based property. In light of this, the following calculations will employ a 6-31G(d) basis on O and the LANL2DZ and Stuttgart basis sets on Cr. Although the Stuttgart and LANL2DZ basis sets provide quite different results, it is likely that a more reliable estimate of $(U-J)$ is obtained with the Stuttgart basis set due to its greater number of basis functions and the fact that some of its basis functions are quite diffuse. This is supported by the agreement between the results obtained with the Stuttgart basis and those calculated with the larger, all-electron Wachters basis set, which is evident from Fig. 3 where the data evaluated with the Wachters basis set essentially overlap those obtained with the Stuttgart basis. This is particularly true when these basis sets are used in conjunction with the 6-31G(d) basis set on oxygen, where the largest discrepancy between the values obtained with the Stuttgart and Wachters basis sets was 0.1 eV for the CrO_6^{9-} system. The importance of employing a flexible, sufficiently diffuse basis set on Cr is discussed further below.

The values in Fig. 3 are not converged with respect to system size. To obtain converged values of $(U-J)$, additional calculations were performed on large clusters using the 6-31G(d) basis on O and either the LANL2DZ or Stuttgart basis sets on Cr. The results of these calculations are summarized in Fig. 4 and demonstrate that $(U-J)$ is converged to within approximately ±0.3 eV or better for clusters larger than $Cr_{11}O_{39}^{45-}$. This is true for both sets of data presented in that figure. Assuming that the Stuttgart basis set provides a more accurate representation of the electronic structure, a converged value of $(U-J)$ is taken as 7.7 eV. This is in line with values previously determined empirically for chromia (4 eV) (Ref. 14) and through constrained DFT+U calculations for Cr in perovskites (7–9 eV).[22]

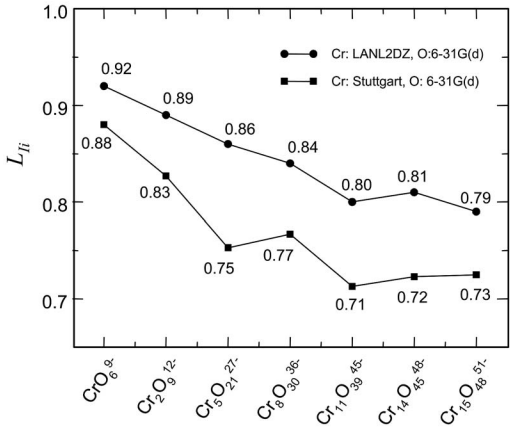

FIG. 5. Dependence of L_{Ii} on the size of the Cr_xO_y clusters for two different basis sets on Cr. The values of L_{Ii} were obtained with Eq. (10), setting I equivalent to the central Cr atom in the cluster. The plotted data were obtained by averaging over the values of L_{Ii} for the three UHF MOs used to evaluate $(U-J)$ in each cluster.

The values of $(U-J)$ evaluated through the UHF calculations are sensitive to both the basis set and the size of the embedded cluster. Analysis of the electronic structure indicates that this dependence is related to the ability of the model to account for the slight degree to which the localized canonical UHF MOs are delocalized over neighboring atoms. To investigate the (de)localized nature of the MOs, the following localization metric is defined:

$$L_{Ii} = \sqrt{\frac{\sum_{\nu=d\text{AO}}^{\text{on } I} c_{\nu i}^2}{\sum_{\nu=\text{all AOs}} c_{\nu i}^2}}, \tag{10}$$

where $c_{\nu i}$ is coefficient of atomic orbital (AO) ν in MO i. This metric measures the contribution of d-type AOs on a specific atom, I, to a particular MO. In the event that $L_{Ii}=1$, it is possible to characterize MO i as being a d orbital that is completely localized on atom I. At the other extreme, i.e., when $L_{Ii}=0$, no d-type AOs on atom I contribute to MO i. In general, the UHF MOs used in the evaluation of $(U-J)$ will lie between these extremes, with values of L_{Ii} that are closer to 1 than to 0.

L_{Ii} values were determined for the UHF MOs used to calculate the data presented in Fig. 3, with a focus on the contribution from AOs centered on the central Cr atom of the cluster, i.e., I=central Cr. The results are plotted in Fig. 5, where each data point represents an average over the L_{Ii} values for each of the three UHF MOs that were localized on the central Cr atom of the cluster and used to evaluate $(U-J)$. The data exhibit trends that are quite similar to the $(U-J)$ values plotted in Fig. 3. Specifically, the values are converged beyond the $Cr_{11}O_{39}^{45-}$ cluster, and the values obtained with the Stuttgart basis set on Cr are lower than those obtained with the LANL2DZ basis set. The convergence of the L_{Ii} values beyond a certain cluster size irrespective of the basis set is consistent with the fact that the orbitals used to calculate $(U-J)$ are only delocalized over a few of the atoms nearest to the central Cr atom, and, hence, adding atoms to the outside of the cluster will have a minimal effect on the results. The differences between the results obtained with the Stuttgart and LANL2DZ basis sets arise from the inclusion of diffuse basis functions in the former, which allow the d states on chromia to more easily interact with orbitals on neighboring atoms, leading to delocalization. The increased delocalization observed with the Stuttgart basis set is consistent with the lower values of $(U-J)$ obtained with this basis. Specifically, delocalization decreases on-site repulsion, yielding lower values for this quantity. Overall, these results indicate that the requisite for obtaining converged values of $(U-J)$ is to employ a structural and theoretical model that adequately accounts for the short-range delocalization of the localized states in the system.

V. DFT+U CALCULATIONS OF BULK CHROMIA

The calculations performed in the previous section led to a converged *ab initio* value of $(U-J)=7.7$ eV. In this section, DFT+U calculations will be performed on bulk-chromia to determine whether this value of $(U-J)$ yields results consistent with experiments. The details of the calculations are given in Sec. V A, and the results are discussed in Sec. V B.

A. Calculation details

DFT+U calculations of bulk chromia were performed with the VASP simulation package.[40,41] The particular DFT+U formalism used in these calculations was that developed by Dudarev *et al.*[17] in which the electron density is optimized to minimize the total energy functional in Eq. (4). For purposes of comparison, calculations were performed for values of $(U-J)$ equal to 0, 2, 4, 6, 7.7, and 8 eV. When $(U-J)=0.0$ eV, the calculation is equivalent to a standard Kohn-Sham DFT calculation. The range of values for $(U-J)$ considered in the calculations is sufficient to examine the dependence of various calculated quantities on the value of $(U-J)$, empirically identify the optimum value of $(U-J)$, and determine if the *ab initio* value of $(U-J)=7.7$ eV yields results consistent with experiments. All calculations were performed on a single hexagonal unit cell of chromia, which is shown in Fig. 6 with labels corresponding to quantities calculated below.

The calculations were performed using two different XC functionals: the LDA functional of Perdew and Zunger[42] and the GGA functional of Perdew-Burke-Ernzerhof (PBE).[43] The nuclei and core electrons were described with the projector augmented wave[44] (PAW) potentials provided with VASP for each of these functionals. The 1*s* electrons on oxygen were included in the core (six valence electron) and the 1*s*, 2*s*, 2*p*, and 3*s* electrons on chromium were described by the PAW potential (12 valence electron). The valence states were described by a set of plane waves expanded up to a kinetic energy cutoff of 550 eV, and a Γ-point-centered $3\times3\times1$ k-point grid was used in all calculations. The fast Fourier transform mesh used to evaluate the augmentation

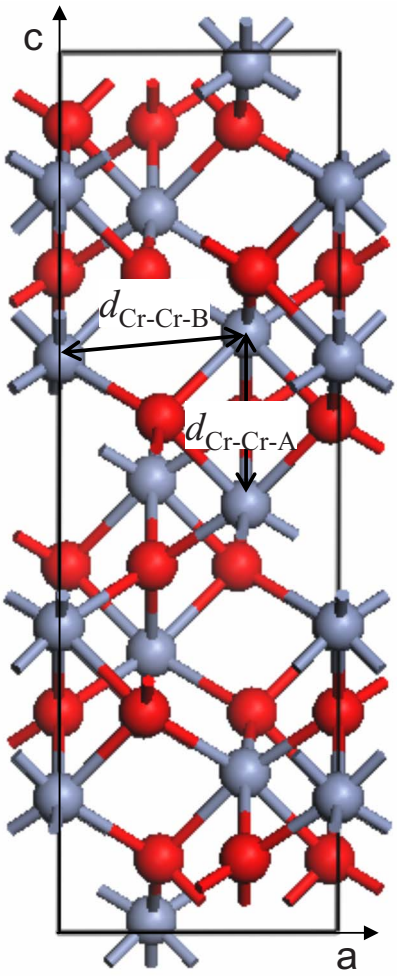

FIG. 6. (Color online) Hexagonal unit cell of chromia. The cell contains six Cr_2O_3 units. The lattice vectors **a** and **c** are labeled, along with the interatomic distances Cr-Cr-A and Cr-Cr-B, which correspond to quantities evaluated below. Chromium atoms are gray and oxygens are red.

charges contained twice the number of grid points along each direction as that used to represent the wave function. This theoretical model converged the total energies to better than 1 meV/atom and the elements of the stress tensor to better than 1 kbar with respect to higher plane wave cutoffs and larger *k*-point grids. Gaussian smearing was used in all optimizations with a smearing width of 0.1 eV. The only deviations from this procedure were in the calculation of the density of states (DOS), band gap, and magnetic moment, where the tetrahedron method[45,46] with corrections by Blöchl *et al.*[47] was used with a Γ-point-centered $9\times9\times3$ *k*-point grid, which increased sampling of the Brillouin zone for the accurate evaluation of the DOS.

The lattice constants and atomic structure of the hexagonal unit cell were optimized as follows. First, a series of systems with different volumes was constructed by altering uniformly the lattice vectors of the experimental hexagonal unit cell of chromia. At each volume, the lattice constants and atomic positions were relaxed, subject to the constraint that the volume remained constant. The lattice constants and atomic positions of the lowest energy structure were optimized further without any constraints placed on the volume of the system, yielding the optimized unit cell and structure. This procedure was performed for both the LDA and PBE functionals over the range of $(U-J)$ values listed above. The results of the optimization provided the optimal lattice constants and atomic structure for each functional and value of $(U-J)$. Furthermore, a set of energy vs volume data was obtained in each case, which provides access to the bulk modulus of the system.

B. Results

Bulk properties of chromia were calculated using the procedure described in the preceding section. The results of these calculations are discussed in what follows and focus on details related to the unit cell (volume and lattice constants), atomic structure (atomic positions and interatomic distances), bulk modulus, and electronic structure (band gap and magnetic moment). Emphasis will be placed on assessing the ability of the *ab initio* value of $(U-J)$ to reproduce experimental results, identifying the optimal empirical value of $(U-J)$ and determining which type of XC functional is better able to provide an accurate description of chromia in DFT+U calculations. This will aid in the development of a model for future calculations of chromia.

1. Unit cell

The unit cell volume and lengths of lattice vectors **a** and **c** are plotted in Fig. 7 as a function of $(U-J)$ for the LDA and PBE functionals along with experimental values.[48] The results demonstrate that the PBE functional provides a reasonable estimate of the volume when $(U-J)=0.0$ eV; however, the volume is severely overestimated when PBE is employed with higher values of $(U-J)$. Meanwhile, LDA underestimates the volume by 7% when $(U-J)=0.0$ eV yet yields results in good agreement with experiment (±2.5%) for values of $(U-J)$ between 2 and 8 eV. In terms of the lattice constants, the PBE functional provides a good estimate of $|\mathbf{a}|$ yet overestimates $|\mathbf{c}|$ by 0.22 Å when $(U-J)=0.0$ eV. The agreement with experiment worsens with this functional as $(U-J)$ is increased. With the LDA functional, both lattice constants are in poor agreement when $(U-J)=0.0$ eV; however, the results are brought in line with experiment as $(U-J)$ is increased. For instance, the calculated value of $|\mathbf{a}|$ agrees to within 1% of the experimentally observed value for $(U-J)$ between 2 and 8 eV, while $|\mathbf{c}|$ agrees with experiment to within 0.5% over the same range of $(U-J)$.

Overall, the results indicate that the LDA functional provides a better description than the PBE functional of the unit cell for finite values of $(U-J)$. Specifically, values of V, $|\mathbf{a}|$, and $|\mathbf{c}|$ that are in good agreement with experiment can be obtained in LDA+U calculations when $(U-J)\approx4.0$ eV. On the other hand, the PBE functional does not yield results where all of these quantities are in good agreement with experiment for a single value of $(U-J)$. The results also indicate that the *ab initio* value of $(U-J)=7.7$ eV yields reasonably accurate values for the unit cell volume and lattice

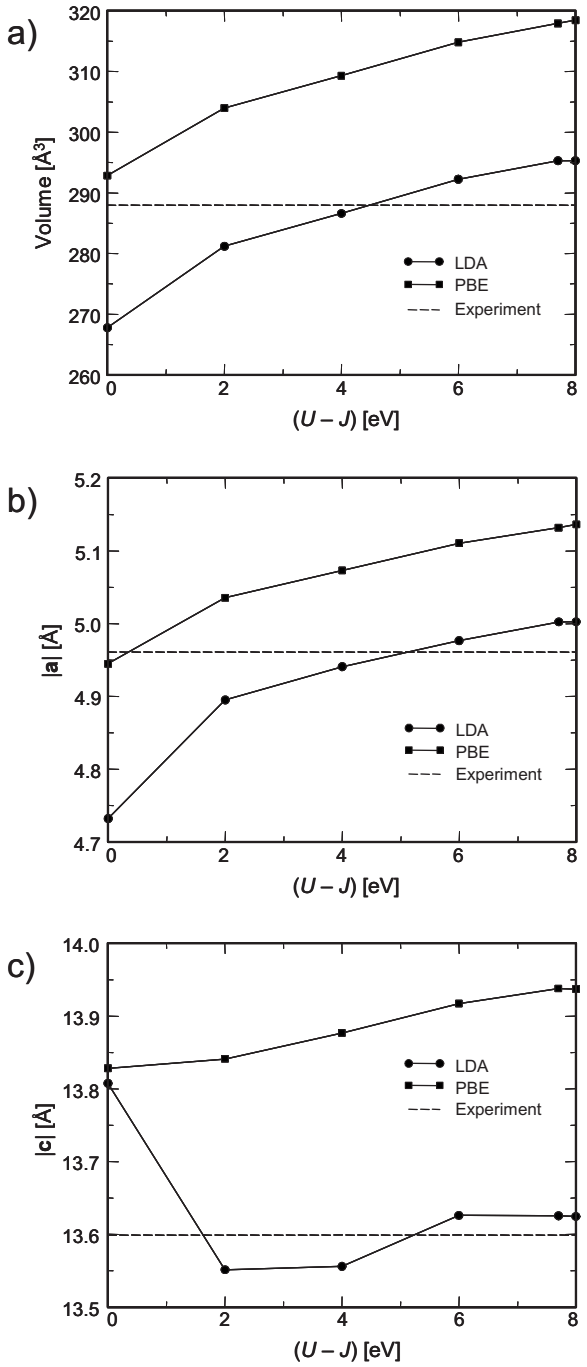

FIG. 7. (a) Volume and lengths of lattice vectors (b) **a** and (c) **c** for the hexagonal unit cell of chromia as a function of $(U-J)$. Data are provided for the LDA and PBE functionals, along with the experimental values of these quantities (Ref. 48).

vectors when used in conjunction with the LDA functional.

2. Atomic structure

Bulk chromia has a corundum structure and belongs to the $R\bar{3}c$ space group, with 6 formula units in the hexagonal cell. The Cr atoms lie along the threefold axis at positions of $\pm(0,0,Z_{\mathrm{Cr}})$ and $\pm(0,0,\frac{1}{2}+Z_{\mathrm{Cr}})$, and the O atoms reside at $\pm(X_{\mathrm{O}},0,\frac{1}{4})$, $\pm(0,X_{\mathrm{O}},\frac{1}{4})$, and $\pm(-X_{\mathrm{O}},-X_{\mathrm{O}},\frac{1}{4})$, where Z_{Cr} and X_{O} are fractions of the lattice vectors.[48] Since these parameters define the positions of the atoms within a given hexagonal unit cell, monitoring their values will shed light on whether changing $(U-J)$ causes significant changes in the fundamental structure of the material. However, since Z_{Cr} and X_{O} are expressed relative to the lattice vectors, they do not provide insight into how the interatomic distances change with $(U-J)$. To explore these changes, the interatomic distances labeled Cr-Cr-A and Cr-Cr-B in Fig. 6 will also be monitored as a function of $(U-J)$. The results of the analysis of the atomic structure are summarized in Fig. 8.

The data in Fig. 8 show that X_{O} decreases with increasing values of $(U-J)$, while Z_{Cr} increases with this parameter. These observations are true for both functionals. The errors in these quantities are relatively large when $(U-J)=0.0$ eV, but the agreement is improved significantly ($\sim$1% relative errors at most) for values of $(U-J)$ between 2 and 8 eV. Overall, these results indicate that the positions of the ions relative to the lattice vectors are not very sensitive to either the XC functional or value of $(U-J)$ used in the calculations. However, the results presented above regarding the unit cell demonstrate that the lattice vectors and volume are sensitive to changes in $(U-J)$. For instance, error associated with the volume ranges from −7% to +2% with the LDA functional as $(U-J)$ is varied from 0.0 to 8.0 eV. The PBE functional overestimates the volume by 2%–11% over the same range of $(U-J)$. Thus, although the positions of the ions relative to the lattice vectors remain relatively constant, the interatomic distances may vary significantly with $(U-J)$. This is reflected in the values of $d_{\mathrm{Cr\text{-}Cr\text{-}A}}$ and $d_{\mathrm{Cr\text{-}Cr\text{-}B}}$ provided in Fig. 8, which indicate that these distances increase with $(U-J)$ for both functionals. When $(U-J)=0.0$ eV, the PBE functional provides an accurate estimate of the interatomic distances, while the agreement with experiment decreases for this functional with higher values of $(U-J)$. Meanwhile, the LDA functional underestimates $d_{\mathrm{Cr\text{-}Cr\text{-}A}}$ and $d_{\mathrm{Cr\text{-}Cr\text{-}B}}$ by 0.13 and 0.14 Å, respectively, when $(U-J)=0.0$ eV, although the results are brought into much better agreement with experiment for larger values of $(U-J)$. Overall, the best simultaneous agreement with experiment for all of the parameters X_{O}, Z_{Cr}, $d_{\mathrm{Cr\text{-}Cr\text{-}A}}$, and $d_{\mathrm{Cr\text{-}Cr\text{-}B}}$ is achieved with the LDA functional when $(U-J)=4.0$ eV, while the *ab initio* value of $(U-J)$ also yields results that are in quite good agreement with the experimental data when used with the LDA functional. The PBE functional again does not yield values of X_{O}, Z_{Cr}, $d_{\mathrm{Cr\text{-}Cr\text{-}A}}$, and $d_{\mathrm{Cr\text{-}Cr\text{-}B}}$ that are all in good agreement with experiment for a specific value of $(U-J)$.

3. Bulk modulus

The bulk modulus B was evaluated by fitting the E vs V data obtained above to a third-order Birch-Murnaghan equation of state.[49,50] The calculated values of B are plotted in Fig. 9 as function of $(U-J)$ for both the LDA and PBE functionals along with the experimental value of this property.[51] The data exhibit a clear distinction between the LDA and PBE values, with the LDA results being in better agreement with experiment over the entire range of $(U-J)$. The large increase in the value of B when moving from $(U$

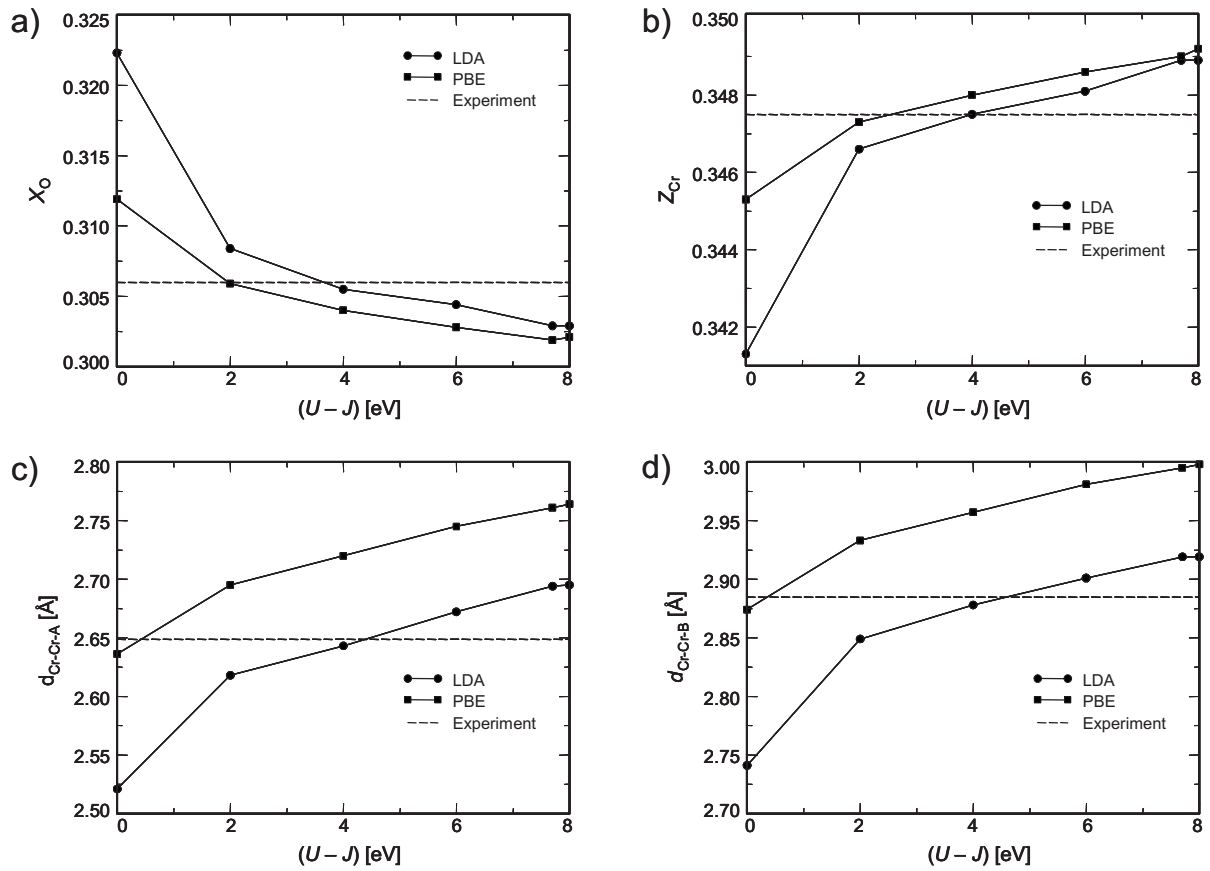

FIG. 8. (a) X_O, (b) Z_{Cr}, (c) $d_{Cr\text{-}Cr\text{-}A}$, and (d) $d_{Cr\text{-}Cr\text{-}B}$ values as a function of $(U-J)$ for the hexagonal unit cell of chromia. The values calculated with the LDA and PBE functionals are shown along with the experimental values for these quantities (Ref. 48).

$-J)=0.0$ eV to $(U-J)=2.0$ eV to with LDA is most likely related to the dramatic change in $|\mathbf{c}|$ mentioned above for the same change in $(U-J)$. Once again, a value of $(U-J)=4.0$ eV used in conjunction with the LDA functional yields results that are most consistent with experimental results; however, the *ab initio* value of $(U-J)$ also provides a good estimate of B with this functional.

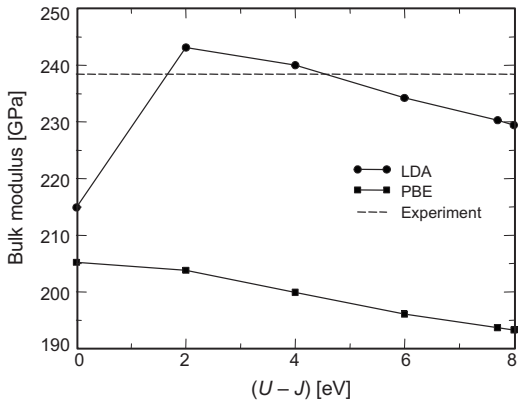

FIG. 9. Bulk modulus of chromia as a function of $(U-J)$. The values calculated with the LDA and PBE functionals are shown along with the experimental value (Ref. 5).

4. Electronic structure

Properties directly related to the electronic structure of the system are most sensitive to the value of $(U-J)$. This is not surprising given that the motivation for the DFT+U technique was to correct for the inability of Kohn-Sham DFT calculations to accurately describe the electronic structure of strongly correlated systems. In the following, the influence of $(U-J)$ on the band gap and magnetic moment will be explored.

The calculated band gap and magnetic moment are plotted in Fig. 10 across the full range of $(U-J)$ values for both XC functionals along with the experimental values.[28–30,52] E_{gap} is underestimated by 2.5 eV with LDA and 1.9 eV with PBE when $(U-J)=0.0$ eV, illustrating the inability of DFT to accurately describe the electronic structure of SCEMs such as chromia. A clear improvement in this quantity is observed for both functionals as $(U-J)$ is increased, and agreement with experiment is obtained for values of $(U-J)$ in the range of 4–6 eV. The *ab initio* value of $(U-J)$ leads to a slight overestimation of the band gap for both functionals. However, the experimental value is based on photoemission/inverse photoemission spectroscopy and thus corresponds to a measure of the difference between the ionization energy and electron affinity. DFT calculations do not directly calculate these properties but approximate them by the Kohn-

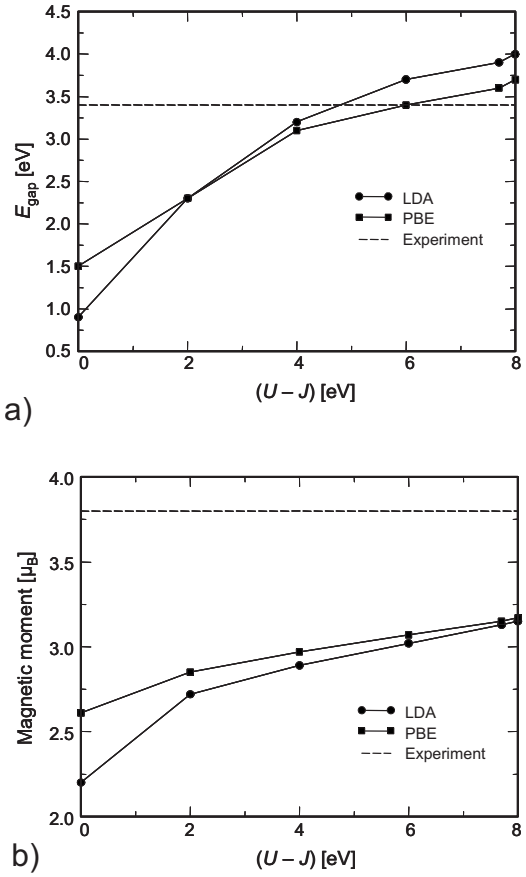

FIG. 10. (a) Band gap and (b) magnetic moment of chromia as a function of $(U-J)$. The values calculated with the LDA and PBE functionals are shown along with the experimental values (Refs. 28–30 and 52).

Sham eigenvalues (Koopman's theorem). This approximation neglects final state effects that will shift the band gap. As such, it is not surprising that calculated band gap differs from the gap derived from photoemission.

The data for the magnetic moment demonstrate that the DFT+U results differ significantly from the experimental results, regardless of the functional or value of $(U-J)$. The discrepancies between the experimental and calculated values may be due to the fact that the experimental value was derived assuming a purely ionic description of chromia, while the calculations and experiments indicate a significant degree of covalent bonding involving the $3d$ electrons of Cr and the $2p$ electrons of oxygen.[52] Such covalent interactions would be expected to reduce the residual magnetic moment on Cr due to the low-spin coupling inherent to chemical bonding, consistent with the lower values we calculate. A re-evaluation of the experimental data incorporating a partially covalent bonding model may result in closer agreement between the calculated and measured values.

5. Summary

The results presented above shed light on how the value of $(U-J)$ and the XC functional in DFT+U calculations affect various bulk properties of chromia. Taken as a whole, the data indicate that superior results are obtained with the LDA functional. That is, using a value of $(U-J)=4.0$ eV in conjunction with LDA yields values for a variety of properties that are in good agreement with experiments. This value for $(U-J)$ had been selected previously through empirical means in a DFT+U study of chromia.[14] Meanwhile, when DFT+U calculations are performed with the PBE functional, there does not exist a single value of $(U-J)$ that simultaneously provides accurate estimates of chromia bulk properties.

The *ab initio* value of $(U-J)=7.7$ eV yields results that are in good agreement with experiment when used with the LDA functional. This is quite remarkable, considering that no experimental information was used in the selection of this particular value of $(U-J)$. As such, the *ab initio* approach outlined above may prove useful in cases where minimal experimental information is available for empirically selecting a value of $(U-J)$.

VI. CONCLUSIONS

In this work, an *ab initio* means of evaluating the parameters $U_{I\ell}$ and $J_{I\ell}$ was developed and tested. This approach rests on an approximate relationship between these parameters and the Coulomb and exchange integrals evaluated in the basis of the UHF MOs corresponding to the localized strongly correlated electronic states. This method does not rely on experimental information and is free of the self-interaction errors inherent in DFT calculations. Thus, the technique developed in this work has clear advantages over the constrained DFT calculations and empirical fitting procedures commonly used to select values of $U_{I\ell}$ and $J_{I\ell}$.

The method was used to evaluate *ab initio* values of $U_{I\ell}$ and $J_{I\ell}$ for the d electrons in chromia, which are localized on the Cr atoms. This was achieved through UHF calculations on embedded Cr_xO_y clusters. The requirements for obtaining converged values of $U_{I\ell}$ and $J_{I\ell}$ were explored, with the key detail being to employ a theoretical and structural model which adequately captures the degree to which the localized states are delocalized over their neighbors. In particular, care must be taken to ensure that the basis set used to represent the valence electrons of the atom on which the localized states reside contains basis functions that are sufficiently diffuse to interact with orbitals on neighboring atoms. A second, more obvious requirement is that the cluster employed in the calculations must be large enough to ensure that the environment in the central portion of the cluster is a good representation of that in the bulk material.

The UHF calculations yielded a converged *ab initio* value of $(U-J)=7.7$ eV for chromia. DFT+U calculations were performed to investigate whether this value was capable of accurately reproducing experimental results. The calculations were performed over a range of values of $(U-J)$ and with two different exchange-correlation functionals. Superior results were clearly obtained with the LDA functional, with a value of $(U-J)\approx 4.0$ eV providing the best agreement with experiment. The results obtained when the *ab initio* value of $(U-J)=7.7$ eV was used with the LDA functional were also in good agreement with experiment, which is quite remark-

able considering that the value of this parameter was determined without any reference to experimental data. The demonstrated ability of the *ab initio* value of $(U-J)$ to yield accurate results is promising for the future application of this technique as a means of unambiguously selecting values of $(U-J)$ for use in DFT+U calculations. This is particularly true for cases in which there is little experimental information available for empirical fitting. Currently, we are using this method to evaluate $(U-J)$ for other transition metal oxides. The results of those calculations will be reported in future publications.

ACKNOWLEDGMENTS

We are grateful to the Army Research Office (E.A.C.) and the Natural Sciences and Engineering Research Council (NSERC) of Canada (N.J.M.) for funding.

*Author to whom correspondence should be addressed; eac@princeton.edu

[1] N. I. Gidopoulos, *Handbook of Molecular Physics and Quantum Chemistry* (Wiley, West Sussex, 2003), Vol. 2, p. 52.
[2] J. Kohanoff and N. I. Gidopoulos, *Handbook of Molecular Physics and Quantum Chemistry* (Wiley, West Sussex, 2003), Vol. 2, p. 532.
[3] F. M. Bickelhaupt and E. J. Baerends, *Reviews in Computational Chemistry* (Wiley-VCH, New York, 2000), Vol. 15, p. 1.
[4] P. Hohenberg and W. Kohn, Phys. Rev. **136**, B864 (1964).
[5] W. Kohn and L. J. Sham, Phys. Rev. **140**, A1133 (1965).
[6] C. Pisani, M. Busso, G. Capecchi, S. Casassa, R. Dovesi, L. Maschio, C. Zicovich-Wilson, and M. Schütz, J. Chem. Phys. **122**, 094113 (2005).
[7] P. Y. Ayala, K. N. Kudin, and G. E. Scuseria, J. Chem. Phys. **115**, 9698 (2001).
[8] J. Hubbard, Proc. R. Soc. London, Ser. A **277**, 237 (1964).
[9] J. Hubbard, Proc. R. Soc. London, Ser. A **281**, 401 (1964).
[10] P. W. Anderson, Phys. Rev. **124**, 41 (1961).
[11] V. I. Anisimov, F. Aryasetiawan, and A. I. Liechtenstein, J. Phys.: Condens. Matter **9**, 767 (1997).
[12] S. L. Dudarev, A. I. Liechtenstein, M. R. Castell, G. A. D. Briggs, and A. P. Sutton, Phys. Rev. B **56**, 4900 (1997).
[13] O. Bengone, M. Alouani, P. Blöchl, and J. Hugel, Phys. Rev. B **62**, 16392 (2000).
[14] A. Rohrbach, J. Hafner, and G. Kresse, Phys. Rev. B **70**, 125426 (2004).
[15] M. Cococcioni and S. de Gironcoli, Phys. Rev. B **71**, 035105 (2005).
[16] V. I. Anisimov and O. Gunnarsson, Phys. Rev. B **43**, 7570 (1991).
[17] S. L. Dudarev, G. A. Botton, S. Y. Savrasov, C. J. Humphreys, and A. P. Sutton, Phys. Rev. B **57**, 1505 (1998).
[18] A. I. Liechtenstein, V. I. Anisimov, and J. Zaanen, Phys. Rev. B **52**, R5467 (1995).
[19] I. V. Solovyev, P. H. Dederichs, and V. I. Anisimov, Phys. Rev. B **50**, 16861 (1994).
[20] V. I. Anisimov, J. Zaanen, and O. K. Andersen, Phys. Rev. B **44**, 943 (1991).
[21] The use of the term localized in this context indicates that the canonical UHF MOs are very atomiclike in nature, and thus localized. It does not imply a unitary transformation of the canonical orbitals to yield a more chemically intuitive electronic structure, which is often called localization.
[22] I. Solovyev, N. Hamada, and K. Terakura, Phys. Rev. B **53**, 7158 (1996).
[23] P. J. Hay and W. R. Wadt, J. Chem. Phys. **82**, 284 (1985).
[24] V. Luana and L. Pueyo, Phys. Rev. B **41**, 3800 (1990).
[25] S. Huzinaga, L. Seijo, Z. Barandiarán, and M. Klobukowski, J. Chem. Phys. **86**, 2132 (1987).
[26] N. W. Winter, R. M. Pitzer, and D. K. Temple, J. Chem. Phys. **86**, 3549 (1987).
[27] N. W. Winter, R. M. Pitzer, and D. K. Temple, J. Chem. Phys. **87**, 2945 (1987).
[28] T. G. Worlton, R. M. Brugger, and R. B. Bennion, J. Phys. Chem. Solids **29**, 435 (1968).
[29] T. R. McGuire, E. J. Scott, and F. H. Grannis, Phys. Rev. **102**, 1000 (1956).
[30] B. N. Brockhouse, J. Chem. Phys. **21**, 961 (1953).
[31] J. Pipek and P. G. Mezey, J. Phys. Chem. **90**, 4916 (1989).
[32] M. S. Gordon and M. W. Schmidt, in *Theory and Applications of Compuational Chemistry: The First Forty Years*, edited by C. E. Dykstra, G. Frenking, K. S. Kim, and G. E. Scuseria (Elsevier, Amsterdam, 2005).
[33] M. W. Schmidt, K. K. Baldridge, J. A. Boatz, S. T. Elbert, M. S. Gordon, J. H. Jensen, S. Koseki, N. Matsunaga, K. A. Nguyen, S. J. Su, T. L. Windus, M. Dupuis, and J. A. Montgomery, J. Comput. Chem. **14**, 1347 (1993).
[34] M. Dolg, U. Wedig, H. Stoll, and H. Preuss, J. Chem. Phys. **86**, 866 (1987).
[35] C. W. Bauschlicher, Jr., S. R. Langhoff, and L. A. Barnes, J. Chem. Phys. **91**, 2399 (1989).
[36] A. J. H. Wachters, J. Chem. Phys. **52**, 1033 (1970).
[37] T. J. Dunning, Jr., J. Chem. Phys. **90**, 1007 (1989).
[38] W. J. Hehre, R. Ditchfield, and J. A. Pople, J. Chem. Phys. **62**, 2921 (1975).
[39] T. J. Dunning, Jr., J. Chem. Phys. **53**, 2823 (1970).
[40] G. Kresse and J. Furthmüller, Comput. Mater. Sci. **6**, 15 (1996).
[41] G. Kresse and J. Hafner, Phys. Rev. B **47**, 558 (1993).
[42] J. P. Perdew and A. Zunger, Phys. Rev. B **23**, 5048 (1981).
[43] J. P. Perdew, K. Burke, and M. Ernzerhof, Phys. Rev. Lett. **77**, 3865 (1996).
[44] P. E. Blöchl, Phys. Rev. B **50**, 17953 (1994).
[45] G. Lehmann and M. Taut, Phys. Status Solidi B **54**, 469 (1972).
[46] O. Jepsen and O. K. Andersen, Solid State Commun. **9**, 1763 (1971).
[47] P. E. Blöchl, O. Jepsen, and O. K. Andersen, Phys. Rev. B **49**, 16223 (1994).
[48] R. E. Newnham and Y. M. de Haan, Z. Kristallogr. **117**, 235 (1962).
[49] F. Birch, Phys. Rev. **71**, 809 (1947).
[50] F. D. Murnaghan, Proc. Natl. Acad. Sci. U.S.A. **30**, 2344 (1944).
[51] L. W. Finger and R. M. Hazen, J. Appl. Phys. **51**, 5362 (1980).
[52] R. Zimmermann, P. Steiner, and S. Hüfner, J. Electron Spectrosc. Relat. Phenom. **78**, 49 (1996).